

Engineered Production of Hapalindole Alkaloids in the Cyanobacterium *Synechococcus* sp. UTEX 2973

Cory J. Knoot,[†] Yogan Khatri,[‡] Robert M. Hohlman,[‡] David H. Sherman,[‡] and Himadri B. Pakrasi^{*,†}

[†]Department of Biology, Washington University, St. Louis, Missouri 63130, United States

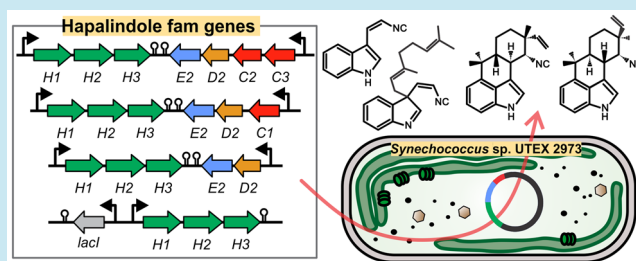
[‡]Life Sciences Institute, University of Michigan, Ann Arbor, Michigan 48109, United States

Supporting Information

ABSTRACT: Cyanobacteria produce numerous valuable bioactive secondary metabolites (natural products) including alkaloids, isoprenoids, nonribosomal peptides, and polyketides. However, the genomic organization of the biosynthetic gene clusters, complex gene expression patterns, and low compound yields synthesized by the native producers currently limits access to the vast majority of these valuable molecules for detailed studies. Molecular cloning and expression of such clusters in heterotrophic hosts is often precarious owing to genetic and biochemical incompatibilities.

Production of such biomolecules in photoautotrophic hosts analogous to the native producers is an attractive alternative that has been under-explored. Here, we describe engineering of the fast-growing cyanobacterium *Synechococcus elongatus* UTEX 2973 to produce key compounds of the hapalindole family of indole–isonitrile alkaloids. Engineering of the 42-kbp “fam” hapalindole pathway from the cyanobacterium *Fischerella ambigua* UTEX 1903 into S2973 was accomplished by rationally reconstructing six to seven core biosynthetic genes into synthetic operons. The resulting *Synechococcus* strains afforded controllable production of indole–isonitrile biosynthetic intermediates and hapalindoles H and 12-*epi*-hapalindole U at a titer of 0.75–3 mg/L. Exchanging genes encoding fam cyclase enzymes in the synthetic operons was employed to control the stereochemistry of the resulting product. Establishing a robust expression system provides a facile route to scalable levels of similar natural and new forms of bioactive hapalindole derivatives and its structural relatives (e.g., fischerindoles, welwitindolinones). Moreover, this versatile expression system represents a promising tool for exploring other functional characteristics of orphan gene products that mediate the remarkable biosynthesis of this important family of natural products.

KEYWORDS: cyanobacteria, natural product, isoprenoid, alkaloid, isonitrile



Cyanobacteria are prolific producers of more than 1000 natural products with potent bioactivities.^{1,2} While a subset of these compounds, including microcystins, is responsible for the harmful effects of algal blooms, many cyanobacterial natural products (cNPs) have promising bioactivities valuable to human health. Genome sequencing of diverse genera of cyanobacteria has revealed a tremendous diversity in the types of encoded biosynthetic gene clusters (BGCs) and identified unique enzymology involved in their production.^{3,4} Genomic studies also highlight that we have still only minimally explored the true metabolic potential encoded by these organisms.² Given that NPs and NP-inspired derivatives constitute roughly half of new pharmaceutical lead compounds,^{5,6} cyanobacteria hold tremendous potential as sources of new bioactive molecules (or core scaffolds) useful to medicine and agriculture. However, ensuring a stable and sufficient production of NPs for characterization is a key limiting step hindering further development.^{5,7–9} These limitations depend on the type of NP but are primarily caused by the slow growth and often challenging culture conditions for environmental strains along with the inherently low

amounts produced in native organisms. Coupling these challenges with difficult purification methods and complex molecular structures can hinder or entirely preclude large-scale chemical synthesis. Accordingly, there have been several reports of expressing cNP genes and gene clusters in heterotrophic^{10–14} and more recently in cyanobacterial hosts^{15,16} in order to gain access to these molecules. In some cases, limitations in non-native substrate pools and cofactors required by specialized NP biosynthetic enzymes can lead to low production yields and/or production of incompletely processed variants in the non-native hosts.^{15,17} Expression of these pathways in related species could overcome some of these limitations owing to more closely matched cofactor availability (e.g., higher NADPH to NADH ratio for redox protein partners), compatibility of genetic elements such as promoters, and similar codon usage.^{18–21} Although traditionally considered slow-growing, some cyanobacterial strains

Received: May 25, 2019

Published: July 8, 2019

exhibit rapid photoautotrophic growth rates (on par with yeast)^{22,23} and thus represent attractive, sustainable production chassis for cNPs.

Hapalindoles are a large family of 80+ polycyclic indole–isonitrile alkaloids produced by branching cyanobacteria of the order *Stigonematales*, obtained from fresh water and terrestrial habitats.²⁴ Many hapalindoles exhibit antibacterial, antimycotic, insecticidal, and cytotoxic activities, sometimes with a potency exceeding that of current clinical therapeutics.²⁴ For instance, hapalindole H is a potent inhibitor of the $\text{Nf-}\kappa\text{B}$ pathway in prostate cancer cells,²⁵ is cytotoxic toward several other malignant lines²⁶ and is active against several important fungal and bacterial pathogens.²⁷ The hapalindole family also includes several related cNP compounds including ambiguines, fischerindoles, hapalindolinones and welwitindolinones that can have different numbers of rings and postassembly structural modifications.^{24,28} BGCs have been mined from over a dozen hapalindole-type cyanobacterial species and the early steps in the biosynthesis of their core ring systems were recently elucidated.^{28–30} Biosynthesis is initiated from *L*-tryptophan, which is converted into *cis* indole–isonitrile and subsequently condensed with geranyl-pyrophosphate (GPP) and cyclized to produce core hapalindoles, fischerindoles, and welwitindolinones (Figure 1).^{29–35} However, much still

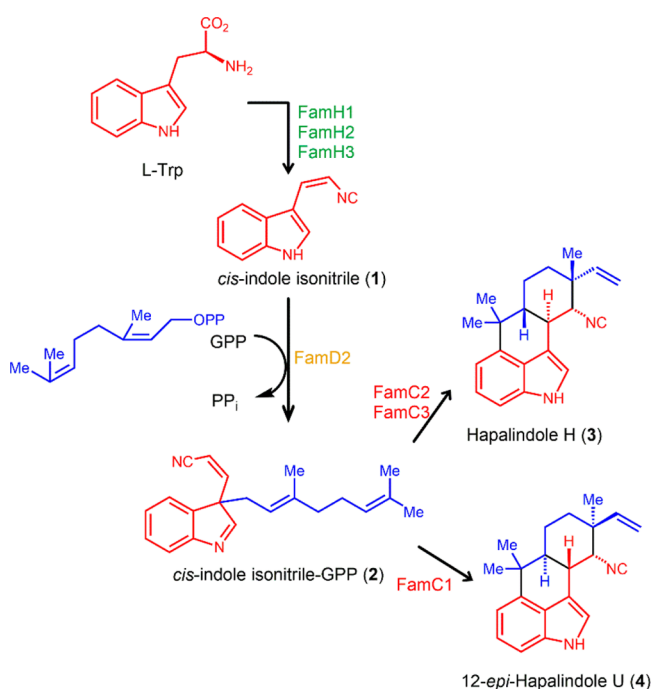


Figure 1. Biosynthesis of *cis* indole–isonitrile (1), prenylated *cis* indole–isonitrile–GPP intermediate (2), and hapalindoles (3,4) from *L*-tryptophan. Enzymes from the hapalindole BGC in *Fischerella ambigua* UTEX 1903 that catalyze each step are indicated.

remains to be understood about the subsequent alkaloid ring expansion mechanism and stereo- and site-specific late-stage tailoring reactions.^{36–38} It is these modifications of the core scaffold that lead to the notable structural diversity observed in hapalindole-type cNPs and modulation of the compound bioactivities.

Here, we report the application of synthetic biology to produce hapalindole-type cNPs in engineered strains of the fast-growing unicellular cyanobacterium *Synechococcus elonga-*

tus UTEX 2973 (S2973).^{22,39} Cloning and rational refactoring of key genes from the 42-kilobase hapalindole *fam* BGC from *Fischerella ambigua* UTEX 1903 afforded controllable photoautotrophic production of *cis* indole–isonitrile, the central geranylated indole–isonitrile intermediate, hapalindole H, and 12-*epi* hapalindole U in S2973 from carbon dioxide (CO₂). Establishment of these foundational strains provides a broad platform to further dissect the unique steps involved in hapalindole biosynthesis and to generate more complex natural and synthetic derivatives using *in vivo* pathway expansion and/or *in vitro* semisynthesis.

RESULTS AND DISCUSSION

Establishment of a Gene Promoter Tool Set for Use in S2973. Before refactoring the *fam* cluster, we worked to identify a set of endogenous and synthetic promoters that we could use to construct multiple synthetic operons, as needed. Reusing genetic elements in a design can result in instability of the construct⁴⁰ and we aimed to avoid this issue by identifying a set of different promoter sequences that are functional in S2973 and that together would provide access to a wide expression range. Furthermore, there have been few reports relating to gene promoter characterization in S2973 and we sought to determine the relative strengths of different promoter elements before including them in our constructs. Thus, we screened a total of 20 native S2973, *Escherichia coli* (*E. coli*), and synthetic promoters for expression in S2973 using enhanced yellow fluorescence protein (eYFP). The promoters tested were chosen based on transcriptomic data for the closely related strain *Synechococcus elongatus* PCC 7942⁴¹ and from a collection of promoters previously used in other cyanobacteria^{42,43} (Table S1). The majority of the native S2973 promoters we tested have not been previously characterized using a reporter gene. Promoter sequences were screened by inserting them upstream of a promoter-less eYFP coding sequence on plasmid pSL3068,⁴⁴ conjugating the vectors into S2973, and measuring the fluorescence of the strains cultured at 38 °C. We included the phycocyanin *cpcB* promoter among the native elements tested but truncated the promoter sequence to remove 218 basepairs from the 5'UTR sequence while retaining the native ribosome binding site (Table S1). This promoter set afforded a roughly 1000-fold eYFP expression range (Figure 2). The synthetic promoters *trc* and J23119 (BioBrick BBa_J23119) resulted in the highest eYFP production, which was roughly 5-fold higher than the truncated P_{*cpcB*}, the strongest native element tested. From this set of promoters, we used P_{*trc*}, P_{*cpcB*}, and P_{J23119} to express the regulatory and hapalindole biosynthetic genes in S2973.

Rational Restructuring of the *fam* BGC and Production of *cis* Indole–Isonitrile in S2973. A subset of hapalindole biosynthetic genes from *Fischerella ambigua* UTEX 1903 (“*fam*” genes) were cloned for expression in S2973. In addition to biosynthetic genes that synthesize the core hapalindole scaffold, the *fam* cluster (Figure 3A) also encodes genes for late-stage tailoring (*famB* genes and *famD1*), tryptophan biosynthesis (*famI* genes) and some genes from the methylerythritol phosphate and shikimate pathways (*famE* genes). Putative transporter (*famA1–3*) and regulatory genes (*famF1* and *F2*) as well as the two *famG* genes remain to be characterized. Hapalindole biosynthesis is initiated with *L*-tryptophan and is converted into the key *cis* indole–isonitrile (1) by the combined action of FamH1, FamH2, and FamH3 enzymes^{29,34} (Figure 1). FamH1 and FamH2 share 62%

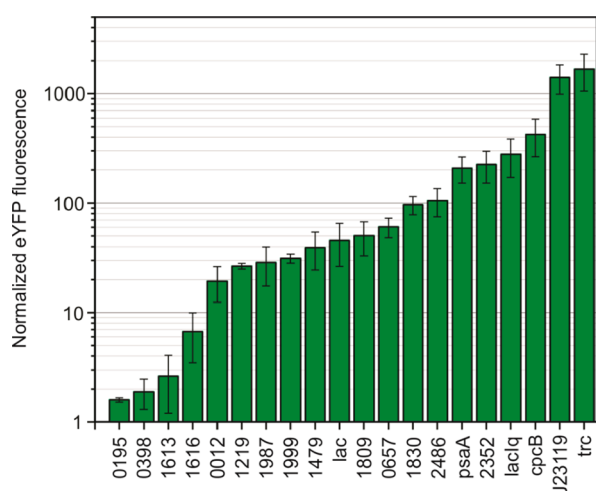


Figure 2. Enhanced yellow fluorescence protein (eYFP) data for 20 promoters characterized in S2973. Fluorescence data were normalized to optical density at 730 nm and are presented as the ratio of this normalized fluorescence to that of a strain carrying the eYFP plasmid without a promoter. Cells were cultured in air under $50 \mu\text{E m}^{-2} \text{s}^{-1}$ fluorescent illumination at 38°C in 250 mL Erlenmeyer flasks. Error bars are 1 SD from the mean derived from at least three biological replicates. Endogenous promoter numbers are named after the corresponding JGI gene locus tag in the closely related cyanobacterium *Synechococcus elongatus* PCC 7942.

sequence identity and are homologues of the isonitrile synthase enzyme PvcA from *Pseudomonas aeruginosa*⁴⁵ while FamH3 is homologous to PvcB and has a fold similar to that of α -ketoglutarate-dependent nonheme iron oxygenases.³⁴ FamH1–FamH3 catalyze the reaction between *L*-tryptophan and ribulose-5-phosphate to generate indole–isonitrile **1**,²⁵ but little is known about the enzyme mechanisms or protein structures. Compound **1** is subsequently prenylated with geranyl pyrophosphate (GPP) by the FamD2 aromatic prenyltransferase to form a second common intermediate.^{29,30} This common prenylated indole–isonitrile–GPP precursor (**2**) is converted into different hapalindoles by cyclase enzymes encoded in the BGCs (*famC* genes).^{30,32,33} The synthetic *fam* operons were designed to express the requisite genes in S2973 on autonomously replicating broad host-range RSF1010 plasmids⁴⁶ (Figure S1). Plasmid assembly is described in the Methods section; primers are listed in Table S2 and strain

genotypes in Table S3. We chose to use plasmids to express the *fam* genes instead of integrating the pathway into the S2973 genome. The primary benefit to using plasmids is that it allows more rapid generation and testing of new constructs and genetic designs because it avoids the necessity to fully segregate strains. The *fam* pathway has not been targeted previously for engineering, and plasmid constructs allowed us to more efficiently screen the different genetic components needed to express and regulate the operons. A secondary reason that we chose an RSF1010-type plasmid is that it can be replicated in a variety of cyanobacterial strains.⁴⁶ This versatility enables future testing of our constructs in other cyanobacteria and comparing them to S2973. However, genome integration typically provides higher strain stability,⁴³ and this option is possible in S2973 using several tools including knock-in suicide vectors with selection markers⁴³ or markerless CRISPR genome editing.⁴⁷

To control production in S2973, the *famH1*, *famH2*, and *famH3* genes were restructured into a single operon under control of the *trc* promoter flanked by two symmetric *lacO* operator sequences (“*trc2O*”, Figure 3B) to enable IPTG induction of gene expression. We initially coexpressed the wild-type *E. coli lacI* repressor protein on the plasmid but this resulted in slow-growing, impaired strains that were not tractable for further experiments. We reasoned that binding of the wild-type *lacI* was insufficient to control transcription from P_{trc2O} and that the strains were compromised owing to product toxicity and/or overconsumption of key metabolic intermediates that stunted growth. Therefore, we used the more tightly binding *lacI* W220F mutant repressor protein⁴⁸ to control expression of the *famH* gene operon in all constructs reported herein. The coding sequence for *lacI* W220F was cloned upstream of the P_{trc2O} -*famH1*–3 operon and the mutant *lacI* gene constitutively coexpressed from P_{J23119} for the hapalindole pathway to be IPTG-inducible (Figure 3B). We only placed *famH1*–*famH3* under an IPTG-inducible promoter, reasoning that controlled induction of the first step in hapalindole biosynthesis would allow us to regulate flux through the downstream steps of the engineered pathway. This operon and regulatory system were cloned and assembled to form plasmid pSL3228. The *E. coli rrnB* T1 terminator sequence downstream of the *famH* operon and a T7 terminator oriented in the reverse direction downstream of *rrnB* T1 is also included in pSL3228. A unique *PmeI* restriction site introduced down-

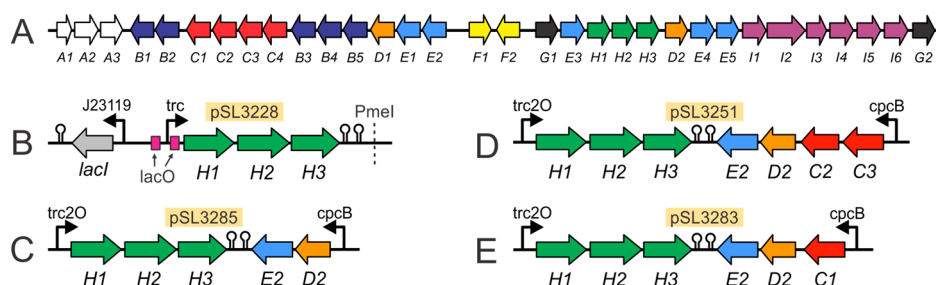


Figure 3. Diagrams of the hapalindole-producing “*fam*” BGC from *Fischerella ambigua* UTEX 1903 and the synthetic *fam* operons constructed on RSF1010 expression plasmids. (A) Diagram of the 42 kilobase pair gene cluster with the 32 *fam* genes. (B) Gene structure of plasmid pSL3228 expressing the *famH* genes and the *lac* repressor mutant W220F (“*lacI*”). The *famH* genes were placed under control of the *trc* promoter surrounded by two *lacO* operator sequences (“*trc2O*”). The *PmeI* (*MssI*) restriction site was used to insert additional *fam* genes in subsequent constructs. (C) Operons on plasmid pSL3285. (D) Operons on plasmid pSL3251. (E) Operons on plasmid pSL3283. The plasmid backbone and the *lacI* cassette is omitted in all panels B–E. Terminators are indicated by black hairpins. Genes under control of the *cpcB* or *J23119* promoter were constitutively expressed.

stream of the T7 terminator was used to later expand the plasmid with additional *fam* genes (Figure 3B). Plasmid pSL3228 was introduced into S2973 by triparental mating to generate strain SL3228.

Organic extracts of freeze-dried SL3228 cell biomass cultured under photoautotrophic conditions revealed production of *cis* indole–isonitrile **1** (Figure 4A,B,C and Figures S2

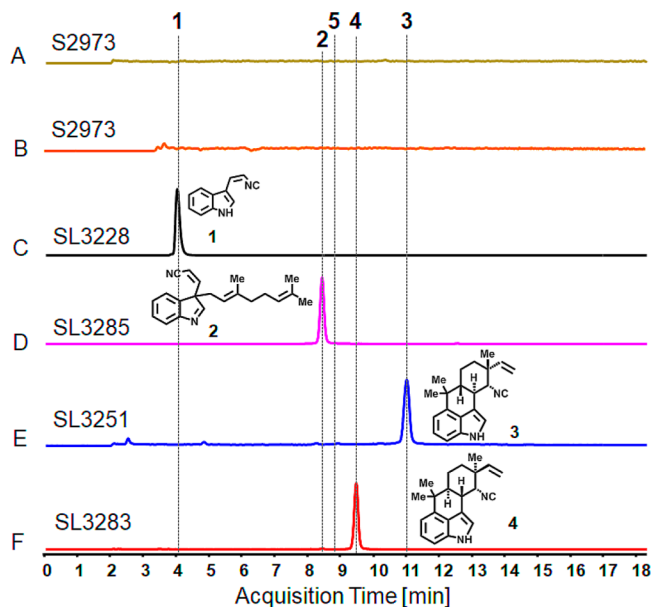


Figure 4. Analysis of isolated hapalindole products generated by engineered strain S2973 using LC–MS. Extracted ion chromatograms (EICs) are shown in all panels. Extracts of wild-type S2973 (A) *m/z* of 168 for *cis* indole–isonitrile (**1**) and (B) *m/z* of 305 for indole–isonitrile–GPP intermediate (**2**) and other hapalindole related compounds. (C) Strain SL3228 engineered to produce **1** (*m/z* of 168). (D) Strain SL3285 produces **2** (*m/z* of 305). (E) SL3251 produces hapalindole H (*m/z* of 305) (**3**). (F) SL3283 produces 12-*epi* hapalindole U (*m/z* of 305) (**4**).

and S3). We also detected production of **1** by SL3228 under uninduced conditions owing to some *trc* promoter leakiness, but this was apparently not sufficient to compromise the strain. Notably, we determined that all three FamH enzymes were required for biosynthesis of **1** in S2973. Strains expressing *famH1* and *famH3* or *famH2* and *famH3* did not produce detectable quantities of **1** (Figure S2). This was surprising as FamH1 and FamH3 alone were shown to be sufficient for *in vitro* production of this molecule.²⁹ We did not detect production of the *trans* **1** isomer in SL3228 under any growth conditions. The *trans* isomer is not converted into hapalindoles according to previous *in vitro* studies.²⁹ On the basis of a comparison to a *cis* **1** HPLC standard curve, we estimate that SL3228 cultured in 60 mL volume in a bioreactor produced 10 $\mu\text{g/g}$ dry cell weight (DCW) when uninduced and 200 $\mu\text{g/g}$ DCW when induced with 75 μM IPTG and cultured under 500 $\mu\text{mol photons} (\mu\text{E}) \text{ m}^{-2} \text{ s}^{-1}$. Growth of SL3228 was negatively impacted by expression of the *fam* genes and the exponential-phase growth rate was reduced by roughly 50% when uninduced compared to a control strain without *fam* genes (Figure S4). Induction with IPTG further reduced the growth rate of the strain to a fraction of the uninduced conditions, and the cells were a deep yellow color distinct from the green color typical of S2973 (Figure S4). We considered

that cells induced with IPTG may be deprived of *L*-tryptophan due to its consumption by FamH1–3. However, we found that *L*-tryptophan content of SL3228 was comparable under induced and uninduced conditions (Figure S5), suggesting that consumption by the *fam* enzymes is compensated by increased biosynthesis of this amino acid.

Production of *cis* Indole–Isonitrile–GPP and Hapalindole H in S2973. Having established that S2973 could generate the precursor *cis* indole–isonitrile, we expanded the biosynthetic pathway by adding the *famD2* prenyltransferase and *fam* cyclase genes into a second operon under control of the S2973 *cpcB* promoter (Figure 3C,D). We chose *cpcB* from the promoter set (Figure 2) because it is the strongest of the native promoter elements tested and we reasoned it would result in comparable expression levels to the IPTG-titratable *trc2O* promoter. The *fam* cluster encodes four cyclases (FamC1–FamC4, Figure 3A) that form homo- and heterodimers to stereospecifically catalyze hapalindole cyclization via a Cope rearrangement.^{32,33} The type of cyclase dimer that catalyzes conversion of the indole–isonitrile–GPP intermediate **2** determines the stereochemistry of the resulting hapalindole.^{30,32,33,35} These cyclases belong to a unique protein family and the first crystal structures of hapalindole cyclases were recently reported by the Sherman group and others.^{33,49} *In vitro* characterization showed that Ca^{2+} ions are required for the activity of some cyclases and that calcium also controls the relative ratio of the hapalindole products generated by their reactions.^{33,35} The enzymes are not known to require other cofactors.

To explore the versatility of our expression system, we constructed two versions of the expanded *fam* pathway on vectors. In the first, we added the *famC2* and *famC3* cyclase genes, *famD2* prenyltransferase gene, and the *famE2* GPP synthase gene (plasmid pSL3251, Figure 3D). In the second we included *famD2* and *famE2*, but omitted the cyclase genes (pSL3285, Figure 3C). The cyclases FamC2 and FamC3 form a heterodimer that converts compound **2** into hapalindole H (**3**, Figure 1).³² FamD2 is an aromatic prenyltransferase that requires Mg^{2+} for activity⁵⁰ and FamE2 is a dedicated GPP synthase that catalyzes the condensation of dimethylallyl pyrophosphate and isopentenyl pyrophosphate to form GPP.²⁹ These plasmids were conjugated into S2973 to generate strains SL3285 and SL3251.

Organic extracts of SL3285 showed conversion of *cis* indole–isonitrile **1** into a new product (**2**, Figure 4C) that possessed the exact retention time of authentic indole–isonitrile–GPP. Product **2** also matched the results obtained by an *in vitro* chemoenzymatic product of synthesized **1** and GPP by purified FamD2 enzyme at various pH values (pH 6.0, 7.8, and 10, Figure 5), as shown before.¹⁸ In addition, the UV-spectrum of product **2** also showed the lack of distinct absorption features at 250–350 nm consistent with dearomatization of the indole ring and loss of intact indolyl vinyl isonitrile group (Figure S6). At mildly acidic pH in the *in vitro* assays, **2** was converted into the C2-prenylated isomer (**5**, Figure 5) that was previously shown to be a terminal shunt metabolite unable to be cyclized into hapalindoles or converted back into compound **2**.³⁰ Importantly, compound **5** was not produced by SL3285 in detectable quantities (Figure 5).

Extracts of SL3251 biomass also expressing the *famC2* and *famC3* cyclase genes contained a new metabolite that was identified as hapalindole H (**3**) using LC–MS, ¹H NMR, and

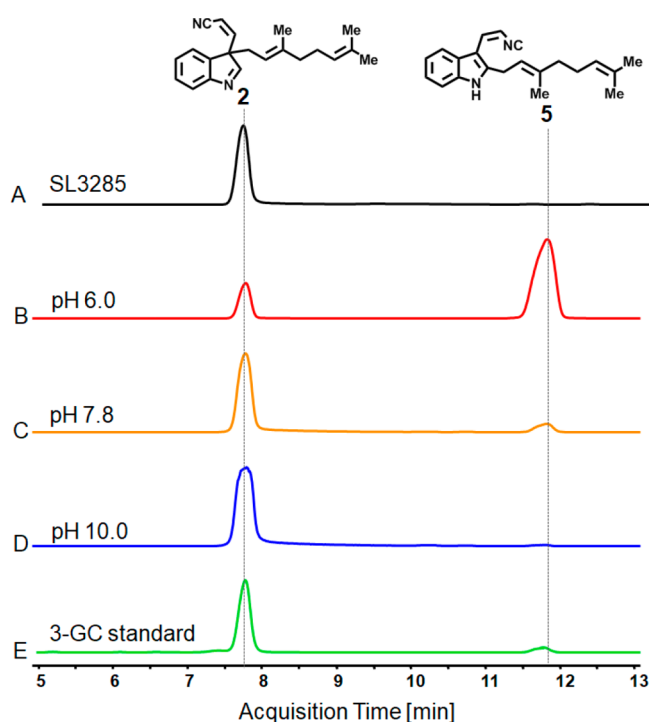


Figure 5. Determination of the indole isonitrile–GPP intermediate isomer produced by engineered SL3285 using LC–MS. EIC trace (m/z of 305) showing the comparison of SL3285 product (A) with the *in vitro* aromatic prenyltransferase assay of purified FamD2 enzyme at pH 6.0 (B), 7.8 (C), and 10 (D) with the substrate **1** and GPP. The authentic indole–isonitrile–GPP (**2**, peak 7.75 min) standard showed that the intermediate produced by SL3285 (and SL3283) is exclusively the C3-geranylated isomer. The C2-geranylated isomer (**5**, 11.8 min) is formed under low-pH conditions but is not generated in S2973.

by comparison to an authentic standard (Figure 4D, S3 and S7 and Table S4). Uninduced SL3251 produced some hapalindole **3** but did not contain detectable amounts of *cis* indole–isonitrile **1** likely due to conversion by the constitutively expressed FamD2 prenyltransferase and FamC2/C3 cyclases (Figure 6A). Titration with IPTG using strain SL3251 indicated that increasing the concentration above 100 μM results in a greater than 75% reduction in S2973 biomass production and accumulation of unreacted **1** in cells (Figure 6B). These data suggest that the $P_{trc20}/lacI$ -W220F regulatory system is titratable and that overinduction of the *fam* pathway incurs a heavy penalty in S2973 biomass production. This may be due to toxicity of the metabolites and/or overconsumption of isoprenoid precursors by FamE2 that are required for pigment and quinone biosynthesis in cyanobacteria.⁵¹ Growth of SL3251 was again reduced compared to a control strain but improved relative to SL3228, particularly under induced conditions with 75 μM IPTG (Figure S4). When induced with 75 μM IPTG and cultured in a bioreactor at 250 $\mu\text{E m}^{-2} \text{s}^{-1}$, SL3251 produced hapalindole **3** at a titer of 1.6–2 mg/g DCW or roughly 2.5–3.1 mg/L. We assessed whether **3** was being secreted from the cells but did not detect this compound or the two intermediates in the culture medium.

We ascertained whether *E. coli* was able to produce hapalindole **3** by screening extracts of cells grown in LB media using HPLC. *E. coli* hosting plasmid pSL3251 induced with 200 μM IPTG contained *cis* indole–isonitrile **1**, but no detectable hapalindole **3** was observed (Figure S8). To test

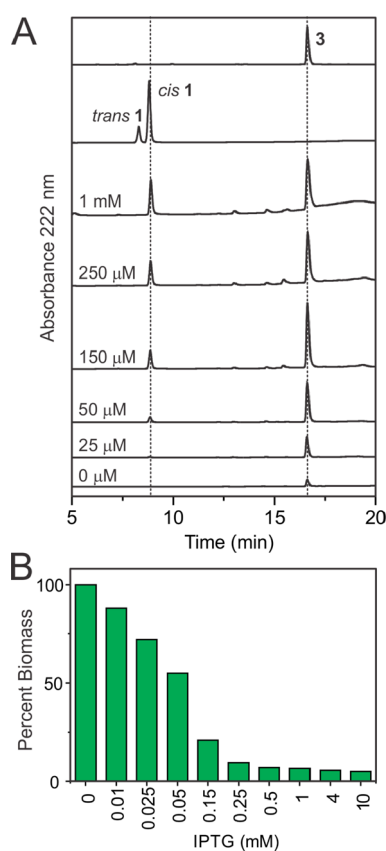


Figure 6. Production of indole–isonitrile (**1**) and hapalindole H (**3**) and dry biomass yield in strain SL3251 as a function of IPTG concentration. (A) HPLC traces of extracts of SL3251 at different IPTG concentrations (labeled). The amount of extract loaded for HPLC was normalized to dry cell biomass. Standards for hapalindole H and indole–isonitrile are shown in the top two traces. (B) Dry biomass yield of SL3251 as a function of IPTG concentration normalized to uninduced biomass yield. Cells were cultured under 400 $\mu\text{E m}^{-2} \text{s}^{-1}$ in a bioreactor bubbling with 5% CO_2 in air. IPTG was added at the start of culturing.

whether the *cpcB* gene promoter incompatibility was responsible for failed production in *E. coli*, we generated another plasmid pSL3325 in which we replaced the cyanobacterial *cpcB* promoter on plasmid pSL3251 with the native *E. coli lac* promoter to drive expression of *famC3*, *famC2*, *famD2*, and *famE2*. IPTG-induced *E. coli* bearing this plasmid remained unable to produce **3**, but again contained unreacted **1** (Figure S8). We did not ascertain whether *E. coli* was able to generate indole–isonitrile–GPP **2**, but previous reports have shown that *E. coli* can produce active FamD2 prenyltransferase.^{30,31} We also used *E. coli* to produce this enzyme for *in vitro* assays (Figure 5). The inability of *E. coli* to synthesize hapalindole H is thus likely due to failed production of active FamC2 and/or FamC3 cyclases.

Production of 12-*epi*-Hapalindole U by Exchanging the Fam Cyclase Genes. We next aimed to establish production of other hapalindole metabolites in S2973 by exchanging FamC2 and FamC3 with another cyclase from the *fam* cluster. Homodimers of the FamC1 cyclase generate 12-*epi*-hapalindole U (Figure 1).³⁰ We exchanged the *famC2* and *famC3* cyclases with the *famC1* gene under control of the *cpcB* promoter to generate strain SL3283 (Figure 3E). Organic extracts of SL3283 induced with IPTG contained 12-*epi*-

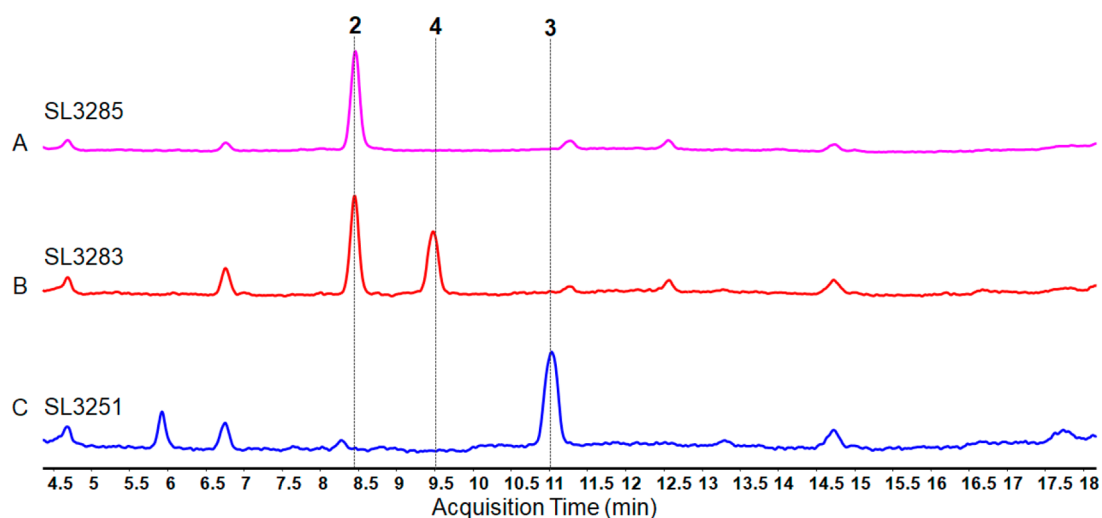


Figure 7. LC–MS traces showing the total ion chromatograms (TICs) of SL3285 (A), SL3283 (B), and SL3251 (C) evidencing unutilized indole–isonitrile–GPP intermediate 2 during the production of 12-*epi*-hapalindole U (4) but not hapalindole H (3).

hapalindole U (4, Figure 4E). Production of hapalindole 4 was confirmed using LC–MS, ^1H NMR, and by comparison to an authentic standard (Figures S3 and S9 and Table S5). In contrast to SL3251, SL3283 also contained unreacted indole–isonitrile–GPP 2 indicating its incomplete conversion into cyclized hapalindole (Figure 7). Overall, yields for hapalindole 4 were lower than those for hapalindole 3 in strain SL3251. In a bioreactor, SL3283 produced 0.7 mg/g DCW 12-*epi*-hapalindole U (0.75 mg/L). Growth of SL3283 in a bioreactor were, like SL3251, improved relative to SL3228 under IPTG-induced conditions (Figure S3). We also tested whether *E. coli* could produce 4 by expressing the FamC1 cyclase alongside FamH1–H3. However, IPTG-induced *E. coli* with plasmid pSL3283 failed to produce detectable levels of hapalindole 4, but rather contained unreacted *cis* indole–isonitrile 1 (Figure S8).

S2973 Hapalindole Yields Compared to Native Producers and Other Engineered Microbes. The S2973 strains reported herein produced roughly 0.7–2 mg hapalindole/g DCW under photoautotrophic conditions. Compared to previous publications, our yields for hapalindole H are slightly below those of the native producer *Fischerella ambigua* or related strains that are reported to yield 4–7 mg/g DCW.^{26,27} The yield of hapalindole U has been reported at near 0.7 mg/g DCW from *Westiellopsis* sp.²⁶ which is on par with our titer for 12-*epi* hapalindole U. Although current yields are comparable to the native producers, S2973 offers distinct advantages over these strains. Depending on the culturing conditions used, we were able to generate dense cultures of S2973 within 3–4 days in a bioreactor, significantly faster than the 6–8 weeks for the native producers.^{26,27} Furthermore, S2973 is genetically tractable with a burgeoning synthetic biology toolset^{22,47,52,53} enabling higher yield potential. For instance, metabolic engineering of the substrate-supplying shikimate⁵⁴ and methylerythritol phosphate pathways⁵¹ alongside central photoautotrophic metabolism^{55,56} are viable strategies to increase titers of the hapalindoles in future S2973 strains. Such genetic tools are currently unavailable for the *Stigonematales* and many other NP-producing cyanobacteria. We compared the current yields of hapalindoles produced by S2973 to those in other cNPs and some plant NPs produced by engineered microbes. Hapalindole yields

were comparable (low mg/g DCW or mg/L range) to those of other NPs in engineered cyanobacteria including shinorine in *Synechocystis*,¹⁶ the nonribosomal peptide lyngbyatoxin A in *Anabaena*,¹⁵ and the plant NPs dhurrin¹⁹ and manoyl oxide¹⁸ in *Synechocystis*. However, S2973 exhibits a faster optimal photoautotrophic doubling time (1.6–2 h) than both *Anabaena* (14 h)¹⁵ and *Synechocystis* (6–7 h).²² The yields in S2973 were 100- to 1000-fold higher compared to some engineered heterotrophic systems including 4-*O*-demethylbarbamide in *Streptomyces venezuelae*¹⁰ and microcystin-LR in *E. coli*¹² (both in the low $\mu\text{g/L}$ range) and comparable to those of microviridins and cyanobactins in *E. coli* (~ 0.2 – 0.7 mg/L).^{11,13} However, significant further strain optimization and metabolic engineering is required to achieve yields commensurate with lyngbyatoxin A produced by engineered *E. coli* (~ 26 mg/L).¹⁴

The Yield-Limiting Step Is Different between the Hapalindole-Producing S2973 Strains. We were able to control the production levels of *cis* indole–isonitrile 1 using the titratable $P_{trc20}/\text{lacI-W220F}$ regulator system (Figure 6). The observation that all of the hapalindole-producing strains grew more quickly than SL3228 upon induction with 50–75 μM IPTG (Figure S4) suggests that 1 is toxic to S2973 when it accumulates in cells. Metabolic burden alone is unlikely to explain the slower growth of the induced strain, as the hapalindole-producing strains SL3251 and SL3283 are also expressing the *famH* genes, cyclase(s), prenyltransferase, and GPP synthase that would be expected to result in an even higher burden. The efficient turnover of *cis* indole–isonitrile is of key importance in improving strain productivity and titer in S2973. Yields of *cis* indole–isonitrile in strain SL3228 were three- or more fold lower than those of the hapalindoles and we reason that the toxicity of this metabolite prevents accumulation of higher amounts in S2973. In contrast, consumption of this intermediate by the constitutively expressed FamD2 and cyclases in strains SL3251 and SL3283 prevents this accumulation, and thus leads to higher yields of the presumably less toxic hapalindoles. Our observations also suggest that the rate-limiting step in the engineered hapalindole pathway is different between the strains. SL3283 accumulated indole–isonitrile–GPP 2 (Figure 7) suggesting that the activities and/or the expression levels of

the cyclases were limiting in this construct. Incomplete conversion of **2** in SL3283 is likely to be responsible for the lower overall yield of 12-*epi* hapalindole U compared to hapalindole H. In contrast, in SL3251, we did not detect any accumulation of **2** (Figure 7), indicating that FamC2 and FamC3 activity or expression level is higher relative to FamC1 in SL3283 and that turnover of **1** by the prenyltransferase FamD2 may be limiting in this strain. Alternatively, this could be due to limitations in the cellular availability of dimethylallyl pyrophosphate in SL3251 that is needed by FamE2 to generate GPP.⁵¹

Rational Refactoring of the Fam Pathway to Direct Biosynthesis and a Means to Study Hapalindole Tailoring. Several reports have shown successful targeting of cNP clusters for heterologous expression in cyanobacteria^{15,16} with the 42-kilobase *fam* cluster, to our knowledge, representing the largest pathway reported so far. Typically, one of the major challenges in working with NP BGCs is that a biosynthetic pathway often results in production of a mixture of possibly dozens of different structural variants. For instance, the *fam* BGC in *Fischerella ambigua* produces primarily hapalindole H but also about 20 derivatives.²⁸ Complex mixtures of these isomers demand arduous fractionation of extracts to purify individual molecules for structural analysis. We used biochemical knowledge of the hapalindole biosynthesis to refactor six to seven genes from the *fam* BGC and thereby direct production toward individual regio- and stereochemically pure hapalindole molecules out of the 20 potential variants.²⁸ Furthermore, the stepwise expansion of the core hapalindole pathway that we established in S2973 provides a powerful approach to determine the role of NP biosynthetic enzymes by inserting single genes with as-of-yet unknown function and analyzing the chemical result. The *fam* BGC and related clusters from other *Stigonematales* encode a variety of tailoring enzymes including cytochrome P450s.²⁸ These monooxygenases can be challenging to express at full activity in *E. coli* or study *in vitro*, but are often active in engineered cyanobacteria due to the presence of compatible reductase partners.^{19–21} Importantly, bioproduction in S2973 did not result in mixtures of pathway intermediates such as the *trans* indole–isonitrile²⁹ or the C2-geranylated shunt product **5** that is produced in chemoenzymatic reactions under pH conditions below 8 (see Figure 5 and reference³⁰). Neither of these compounds are substrates for conversion into hapalindoles. The stereo- and regio-specificity of the *in vivo* S2973 production system provides distinct advantages for scale-up and gene-function studies compared to *in vitro* or synthetic chemical production methods for hapalindoles. We observed that *E. coli* accumulated *cis* indole–isonitrile but was unable to produce the hapalindoles. This is likely due to its inability to process the N-terminal transmembrane region of *fam* cyclases.³²

CONCLUSIONS

We established a photoautotrophic production system for key members of the hapalindole cNP family as well as critical biosynthetic intermediates in a fast-growing heterologous cyanobacterial host. Historically, bioengineering of cyanobacteria has focused on the production of “low-cost, high-volume” commodity chemicals and biofuels.⁵⁶ Although improvements in engineering strategies and a better understanding of photoautotrophic metabolism have yielded significant increases in cyanobacterial titer and productivity,⁵³ the need to

compete with cheap petrochemical-derived fuels and chemicals currently prevents these strains from being economically viable. Photosynthetic production of complex ‘high-cost, low-volume’ compounds such as NPs could overcome this type of direct economic competition. Our S2973 strains demonstrate that fast-growing unicellular cyanobacteria are a promising production chassis for CO₂-derived NP compounds that are challenging to produce in *E. coli* or via chemical synthesis. The two hapalindole variants that we produced have useful bioactivities including antibacterial and antifungal properties and toxicity against malignant cell lines.^{24,27} Moreover, these strains serve as a foundation for future engineering to improve hapalindole titers and as a means to dissect the fascinating biochemical transformations involved in the biosynthesis of this family of compounds. Once the tailoring steps of the *fam* pathway (and other hapalindole pathways) are more clearly understood, S2973 strains can be engineered to produce more complex hapalindoles or generate entirely novel derivatives by combinatorially expressing tailoring genes from other *Stigonematales* species. The inability of *E. coli* to produce the hapalindoles illustrates that heterotrophs are poor expression hosts for the critical Fam cyclase enzymes. This provides an impetus to further develop cyanobacteria as expression platforms for these types of pathways. Improvements in cyanobacterial synthetic biology provides a means to study both known cNP clusters as well as the hundreds of cryptic cNP biosynthetic pathways that remain to be explored.^{2,4} This could provide access to entirely new classes of cNPs and a means to explore the rich diversity of fascinating chemical transformations involved in their assembly and structural diversification.

METHODS

Cyanobacterial Culturing and Conjugation. S2973 was maintained on BG11 plates or liquid media at 38 °C. Kanamycin was added to a concentration of 10 μg/mL on plates and in liquid when required. Strains were routinely cultured in 250 mL shaker flask under 50–150 μmol photons (μE) m⁻² s⁻¹ or in a MC1000 multiculter bioreactor (Photon Systems Instruments, psi.cz) under 200–900 μE m⁻² s⁻¹ LEDs while bubbling with 5% CO₂-supplemented air. Expression plasmids were introduced into S2973 via triparental mating with an *Escherichia coli* strain hosting the Inc.P helper plasmid pRL443 and with another hosting the plasmid to be introduced into S2973. For mating, S2973 was cultured overnight to an O.D. 730 nm of 0.3–0.6 and *E. coli* were cultured overnight in LB media. Cells were collected by centrifugation, washed twice with deionized water, mixed, and spread on nitrocellulose membranes (Millipore Immobilon-NC) then placed on BG11 agar plates with 5% (v/v) LB. After outgrowth for 1 day at 38 °C in air, membranes were moved to BG11 plates with 50 μg/mL kanamycin. Ex-conjugants were individually picked and moved to BG11 plates with 10 μg/mL kanamycin and PCR genotyped to confirm transfer of the plasmid. To mitigate issues with strain instability, we resurrected strains from –80 °C frozen stocks (with 10% v/v DMSO as cryoprotectant) roughly every two months. We did not add additional calcium to the media when culturing the hapalindole-producing strains (unmodified BG11 contains 250 μM Ca²⁺).

Construction of eYFP and *fam* Expression Vectors. All plasmids were constructed using Gibson Assembly.⁵⁷ PCR primers used to amplify the promoters, *fam* genes and other

genetic elements are listed in [Supplementary Table S2](#). All vectors described herein were derived from pVZ321, a RSF1010 broad host-range plasmid,⁴⁶ and maps for these constructs are shown in [Figure S1](#). To screen the promoter activity using eYFP, we used plasmid pSL3068 that was described previously.⁴⁴ Promoters were amplified from S2973 or *E. coli* genomic DNA (gDNA) isolated using phenol/chloroform extraction and ethanol precipitation. To assemble the promoter-eYFP constructs, pSL3068 was linearized using AarI restriction enzyme, gel-purified using a Purelink Quick Gel Extract kit (Thermo Fisher), and mixed with the PCR-amplified promoters for Gibson Assembly. The following primers were used to PCR-amplify the promoter regions for Gibson assembly: 0012, P0012-F/P0012-R; 0195, P0195-F/P0195-R; 0398, P0398-F/P0398-R; 0657, P0657-F/P0657-R; 1219, P1219-R/P1219-R; 1479, P1479-F/P1479-R; 1613, P1613-F/P1613-R; 1616, P1616-F/P1616-R; 1809, P1809-F/P1809-R; 1830, P1830-F/P1830-R; 1987, P1987-F/P1987-R; 1999, P1999-F/P1999-R; 2352, P2352-F/P2352-R; 2486, P2486-F/P2486-R; *cpcB*, P*cpcB*-F/P*cpcB*-R; J23119, P*J23119*-F/P*J23119*-R; *lac*, P*lac*-F/P*lac*-R; *lacIq*, P*lacIq*-F/P*lacIq*-R; *psaA*, P*psaA*-F/P*psaA*-R; *trc*, P*trc*-F/P*trc*-R. These primers amplified the native ribosome binding site along with the promoter region. The assembly reactions were transformed into XL1-Blue *E. coli* and plated on LB with 50 $\mu\text{g}/\text{mL}$ kanamycin overnight. Resistant colonies were selected for culturing in LB liquid media. Plasmids were isolated using a GeneJet Plasmid Miniprep kit (Thermo Scientific), and correct sequences were verified using Sanger sequencing (Genewiz, www.genewiz.com). Correctly assembled plasmids were introduced into S2973 using triparental mating.

To construct the *fam* expression plasmids, we generated a derivative vector pSL3084 from the RSF1010 plasmid pSL3067.⁴⁴ pSL3084 has the direct repeat region around the *aphA* kanamycin resistance cassette removed in order to improve vector stability. pSL3084 was used as the backbone/parent plasmid to generate the *fam* plasmids. The pSL3084 fragments were amplified using the two primer pairs 3084-1F/3084-1R and 3084-2F/3084-2R from the pSL3067 template, and the two purified fragments were joined using Gibson assembly. To assemble the *fam* plasmids, pSL3084 was digested with *Xba*I restriction enzyme (Thermo) and purified, and this linearized vector was used in Gibson Assembly reactions with PCR products amplified from *Fischerella ambigua* UTEX 1903 gDNA or the promoter-eYFP plasmids unless otherwise noted.

To assemble pSL3228, the PCR fragments were amplified with 28–30 bp terminal overhangs or directly synthesized prior to Gibson assembly with *Xba*I-digested pSL3084: the J23119 promoter and *lacI* W220F cassette synthesized with terminal overlaps for Gibson assembly (see [Supporting Information](#)); the *trc* promoter sequence was also synthesized with overlaps (see [Supporting Information](#)); *famH1* was amplified using CK142/CK065 primers; *famH2* and *famH3* were amplified using CK066/CK112 primers; and the bidirectional terminator was amplified using CK113/CK143 primers and cloning vector pSR26-2⁵⁸ as a template. These five fragments were mixed with *Xba*I-digested pSL3084 for Gibson assembly. CK143 also introduced a unique *Pme*I (*Mss*I) enzyme restriction site downstream of the terminator useful for future cloning. To make plasmids pSL3251, pSL3283, and pSL3285, pSL3228 was digested with *Pme*I, gel-purified, and used as a linearized backbone for Gibson assembly. The PCR

fragments for pSL3251 were amplified using the following primers: *famE2*, CK213/CK170; *famD2*, CK171/CK073; *famC2*, CK074/CK075; *famC3*, CK076/CK041; *cpcB* promoter, CK037/CK077. pSL3283 PCR fragments for assembly were amplified using these primers: *famE2* and *famD2*, CK213/CK214 using pSL3251 DNA template; *famC1*, CK215/CK216; *cpcB* promoter, CK217/CK172. Primers for generating pSL3285 PCR fragments were as follows: *famE2* and *famD2*, CK213/CK188; *cpcB* promoter, CK189/CK172. Primers amplifying the start codon of the *fam* genes were designed to engineer the RBS for higher translation rates using RBS calculator v2.0 (<https://salislab.net/software/forward>).⁵⁹ The input target translation initiation rate (TIR) using RBS calculator was 5000. To generate plasmid pSL3325 replacing the *cpcB* with the *lac* promoter the following primers were used: the *famE2*, *D2*, *C2*, and *famC3* fragment were amplified from pSL3251 using CK213/CK270 primers and the *lac* promoter was amplified from the P_{lac}-eYFP plasmid using primers CK271/CK272. After Gibson assembly, plasmids were propagated in *E. coli*, isolated, and Sanger sequenced to ensure correct assembly as described for the eYFP plasmids above.

Fluorescence Measurements. Fluorescence from S2973 strains was measured when the cultures were in the early to middle linear growth phase (optical density at 730 nm between 0.2–0.6). For these experiments, cells were cultured at 38 °C in air in 250 mL glass shaker flasks under 50 $\mu\text{E m}^{-2} \text{s}^{-1}$ fluorescent lights. O.D.s and fluorescence were measured for 150 μL of culture in 96-well plastic trays using a Bio-Tek μQuant Plate Reader. Fluorescence measurements were made using an excitation wavelength of 514 nm, and emission was monitored at 527 nm.

Analysis and Purification of Hapalindoles from S2973 Biomass. The biosynthesized compounds in S2973 were isolated by macerating 20 mg of the corresponding biomasses in 5 mL of extraction solvent (1:1 mixture of dichloromethane and methanol) using Tissue Tearor (BioSpec Products Inc.) for 10 min. The extract was centrifuged at 8200 rpm for 15 min, and the pellet was re-extracted once. The pooled organic extract was dried in a nitrogen stream and dissolved in 400 μL of methanol, and 1 μL of the extract was analyzed either in Q-TOFF or TOFF as described below in the *in vitro* chemoenzymatic method. For the structural elucidation, 500 to 700 mg of the corresponding biomass was macerated in 10 mL of the extraction solvent, and extracted twice. The extracted products were dried and concentrated as before and purified by HPLC (Column: XBridge™ Prep Phenyl 5 μM , 10 \times 250 mm), using a 60–100% gradient of acetonitrile in water over 28 min. The purified compounds were concentrated, dissolved in C₆D₆, and analyzed using a Varian 600 MHz NMR spectrometer. Proton and carbon signals are reported in parts per million (δ) using residual solvent signals as an internal standard.

Expression and Purification of FamD2. The expression and purification of FamD2 was performed as described.³⁰ Briefly, a single BL21(DE3) colony of FamD2 transformant was inoculated in LB medium containing 50 $\mu\text{g}/\text{mL}$ kanamycin and grown overnight at 37 °C shaking at 200 rpm. The main culture (1 L) was prepared at the dilution of 1:100 in 2.8 L of Fernbach flask containing LB medium and the same concentration of antibiotic. The cells were grown (37 °C, 200 rpm) to an optical density (A600 nm) of 0.6. The culture flasks were chilled in ice, were induced with IPTG (0.2 mM), and were further incubated (16 °C, 200 rpm) for 16 h.

The cells were harvested (5000 rpm, 4 °C, 15 min), flash frozen, and stored at –80 °C until purification. The cell pellets were resuspended at 4 °C in the lysis buffer (10 mM HEPES, 50 mM NaCl, 0.2 mM TCEP, 10% glycerol), containing 0.5 mg/mL of lysozyme and 1 μ L of benzonase. The mixture was stirred for 30 min and sonicated on ice for 100 s total time using 10 s pulses followed by a 50 s pause. The cellular debris was removed by centrifugation (35 000 rpm, 4 °C, 35 min). Imidazole (10 mM) was added in the clarified lysate and loaded onto Ni-NTA agarose column equilibrated with lysis buffer. The column was washed with five column volume of wash buffer (10 mM HEPES, 300 mM NaCl, 0.2 mM TCEP, 10% glycerol, 20 mM imidazole) and the His-tagged protein was eluted with elution buffer (10 mM HEPES, 50 mM NaCl, 0.2 mM TCEP, 10% glycerol, 300 mM imidazole). The fractions were pooled and dialyzed using a PD10-desalting column (GE Healthcare) using lysis buffer (10 mM HEPES, 50 mM NaCl, 0.2 mM TCEP, 10% glycerol). The purified protein was analyzed by SDS-PAGE gel for purity, measured by Nanodrop for concentration, and flash-frozen in liquid nitrogen to store at –80 °C.

Synthesis of Geranyl Diphosphate Triammonium Salt. The synthesis was previously described.⁶⁰ Briefly, in a 10 mL round-bottom flask purged with nitrogen, tris (tetrabutylammonium) hydrogen pyrophosphate (1.33 g, 1.39 mmol) was dissolved in CH₃CN (1.50 mL). Geranyl chloride (0.12 mL, 0.63 mmol) was added, and the reaction mixture was stirred at room temperature for 2 h.

Synthesis of (Z)-2-(3-Indolyl)vinyl Isocyanide (cis Indole–Isonitrile). The synthesis was previously described.⁶⁰ Briefly, to a 50 mL two-neck round-bottom flask purged with nitrogen at –78 °C (dry ice/acetone), diethyl (isocyanomethyl) phosphonate (0.20 mL, 1.248 mmol) was diluted with THF (5 mL). KHMDS (1 M THF, 2.60 mL, 2.60 mmol) was added dropwise, and the reaction was stirred at –78 °C for 30 min. To a separate 4 mL vial, indole-3-carboxaldehyde (164 mg, 1.13 mmol) was dissolved in THF (5 mL), and the resulting solution was added dropwise to the KHMDS solution at –78 °C. The resulting mixture was stirred at 0 °C (cryocool) for 21 h. The resulting red solution was quenched by the addition of AcOH (0.15 mL, 2.6 mmol) and concentrated. The dark red residue was diluted with EtOAc (20 mL), washed with 1 M aqueous potassium phosphate buffer (20 mL, pH 7), washed with brine, dried with Na₂SO₄, and concentrated to a dark red oil. The residue was dissolved in Et₂O and purified by flash chromatography (24%–100% pentane/Et₂O, SiO₂) to afford the titled compound as a red crystalline solid (20.7 mg, 10.8%). Spectral data were in accord with those reported.⁶⁰

¹H NMR (599 MHz, CDCl₃) δ : 5.75 (d, *J* = 8.8 Hz, 1H), 6.80 (dt, *J* = 9.1, 4.6 Hz, 1H), 7.23 (t, *J* = 7.5 Hz, 1H), 7.27–7.30 (m, 1H), 7.44 (d, *J* = 8.1 Hz, 1H), 7.68 (d, *J* = 7.9 Hz, 1H), 8.14 (d, *J* = 2.8 Hz, 1H), 8.61 (s, 1H). ¹³C NMR (151 MHz, CDCl₃) δ 168.45, 135.03, 126.76, 126.41, 124.16, 123.19, 120.93, 118.00, 111.50, 110.08, 104.4 (t).

In Vitro Aromatic Prenyltransferase FamD2 Assay. The *cis* indole–isonitrile and GPP were synthesized as described above and the aromatic prenyltransferase FamD2 was used to generate the indole–isonitrile–GPP intermediate *in vitro*. The *in vitro* assay was performed in a 50 μ L reaction containing FamD2 (10 μ M), indole isonitrile (1 mM), GPP (1 mM), and MgCl₂ (20 mM), either in 50 mM PIPES buffer, pH 6.0, or 50 mM Tris buffer, pH 7.8 or 50 mM glycine buffer, pH

10.0. The reaction was incubated at 30 °C for 2 h and quenched and extracted twice with a double volume of ethyl acetate. The organic layer was combined, dried, and reconstituted in 50 μ L of acetonitrile for LC–MS analysis. The analytical scale liquid chromatography–mass spectrometry (LC–MS) run was performed on an Agilent G6545A quadrupole-time-of-flight (Q-TOF) or Agilent 6230 time-of-flight (TOF) mass spectrometer equipped with a dual AJS ESI source and an Agilent 1290 Infinity series diode array detector, autosampler, and binary pump. An XBridge Shield RP18 3.5 μ m, 3.0 mm \times 150 mm from Waters was used for all separations. The chromatographic method for all substrate gradients was from 60% to 100% of 95% acetonitrile water containing 0.1% formic acid over 27 min. A volume of 1 μ L injections was made for each sample.

Dowex 50WX8 Resin Preparation and GPP Purification. Dowex 50WX8 resin (26 g, hydrogen form) was washed with half saturated aqueous ammonium chloride (5 \times 50 mL) and water (5 \times 50 mL) until the pH of the supernatant equaled 5. The slurry was rinsed twice with ion exchange buffer (2% isopropyl alcohol in 25 mM aqueous ammonium bicarbonate) and loaded into a flash column and equilibrated with ion exchange buffer. The reaction mixture was concentrated to afford an orange residue which was diluted with ion exchange buffer. The crude mixture was chromatographed with two column volumes of ion exchange buffer (75 mL) over Dowex 50WX8 resin previously prepared. The fractions were combined and concentrated by rotary evaporation, flash frozen, and lyophilized for 2d. The resulting white powder was diluted with 0.1 M ammonium bicarbonate (4 mL) and 50% isopropyl alcohol/CH₃CN (10 mL), vortexed for 30 s, and centrifuged (2000 rpm, room temperature for 5 min). The organic layer was extracted, and the residual 0.5 mL of yellow liquid was diluted with 50% isopropyl/CH₃CN and this process was repeated twice. The combined organic layers were concentrated to afford a white solid (360 mg). The white solid was taken up in 50% isopropyl/25% CH₃CN/25% 0.1 M aqueous ammonium bicarbonate and chromatographed over cellulose. The resulting fractions were combined and lyophilized affording the titled compound as a white powder (126.4 mg, 54.7%).

¹H NMR (400 MHz, D₂O/ND₄OD) δ : 1.92 (d, *J* = 1.3 Hz, 3H), 1.98 (s, 3H), 2.01 (d, *J* = 1.3 Hz, 3H), 2.39 (d, *J* = 6.5 Hz, 2H), 2.41–2.49 (m, 2H), 5.45–5.53 (m, 1H), 5.74 (dt, *J* = 6.1, 3.9 Hz, 1H). ¹³C NMR (151 MHz, D₂O/ND₄OD) δ : 142.46, 133.67, 124.40, 120.46, 62.61, 39.10, 25.92, 25.16, 17.26, 15.89. ³¹P NMR (162 MHz, D₂O/ND₄OD) δ –9.93 (d, *J* = 21.6 Hz), –6.08 (d, *J* = 21.6 Hz).

■ ASSOCIATED CONTENT

● Supporting Information

The Supporting Information is available free of charge on the ACS Publications website at DOI: 10.1021/acssynbio.9b00229.

Plasmid maps, NMR spectra, LC–MS data with standards, strain growth in bioreactor, analysis of *L*-tryptophan content, tables of promoter sequences, primers used in plasmid construction, strain genotypes, and ¹H NMR shifts for hapalindoles (PDF)

AUTHOR INFORMATION

Corresponding Author

*Email: pakrasi@wustl.edu.

ORCID

Cory J. Knoot: 0000-0002-8103-6093

Yogan Khatri: 0000-0002-2432-7679

David H. Sherman: 0000-0001-8334-3647

Himadri B. Pakrasi: 0000-0001-8240-2123

Author Contributions

C.K., Y.K., D.H.S., and H.B.P. designed the overall project. C.K. designed, constructed, and tested the S2973 strains and characterized metabolites using HPLC. Y.K. and R.H. purified products from S2973, analyzed compounds using LC–MS and NMR, and performed the *in vitro* enzymatic assays.

Notes

The authors declare no competing financial interest.

ACKNOWLEDGMENTS

We thank all members of the Pakrasi and Sherman groups for collegial discussions. Studies in the Pakrasi lab were supported by a Postdoctoral Fellowship from the Arnold and Mabel Beckman Foundation (Irvine, CA) to Cory Knoot. NIH (R35 GM118101) and the Hans W. Vahlteich Professorship are gratefully acknowledged for financial support (to D.H.S.).

ABBREVIATIONS

S2973, *Synechococcus elongatus* UTEX 2973; NP, natural product; cNP, cyanobacterial natural product; GPP, geranyl pyrophosphate; BGC, biosynthetic gene cluster; *fam*, 42-kbp hapalindole gene cluster from *Fischerella ambigua* UTEX 1903; eYFP, enhanced yellow fluorescence protein; DCW, dry cell weight

REFERENCES

- (1) Burja, A. M., Banaigs, B., Abou-Mansour, E., Grant Burgess, J., and Wright, P. C. (2001) Marine cyanobacteria - a prolific source of natural products. *Tetrahedron* 57, 9347–9377.
- (2) Dittmann, E., Gugger, M., Sivonen, K., and Fewer, D. P. (2015) Natural Product Biosynthetic Diversity and Comparative Genomics of the Cyanobacteria. *Trends Microbiol.* 23, 642–652.
- (3) Kehr, J. C., Picchi, D. G., and Dittmann, E. (2011) Natural product biosyntheses in cyanobacteria: A treasure trove of unique enzymes. *Beilstein J. Org. Chem.* 7, 1622–1635.
- (4) Kleigrewe, K., Gerwick, L., Sherman, D. H., and Gerwick, W. H. (2016) Unique marine derived cyanobacterial biosynthetic genes for chemical diversity. *Nat. Prod. Rep.* 33, 348–364.
- (5) Butler, M. S. (2004) The Role of Natural Product Chemistry in Drug Discovery. *J. Nat. Prod.* 67, 2141–2153.
- (6) Newman, D. J., and Cragg, G. M. (2016) Natural Products as Sources of New Drugs from 1981 to 2014. *J. Nat. Prod.* 79, 629–661.
- (7) Cragg, G. M., Schepartz, S. A., Suffness, M., and Grever, M. R. (1993) The Taxol Supply Crisis. New NCI Policies for Handling the Large-Scale Production of Novel Natural Product Anticancer and Anti-HIV Agents. *J. Nat. Prod.* 56, 1657–1668.
- (8) Paterson, I., and Anderson, E. A. (2005) The Renaissance of Natural Products as Drug Candidates. *Science* 310, 451.
- (9) Marienhagen, J., and Bott, M. (2013) Metabolic engineering of microorganisms for the synthesis of plant natural products. *J. Biotechnol.* 163, 166–178.
- (10) Kim, E. J., Lee, J. H., Choi, H., Pereira, A. R., Ban, Y. H., Yoo, Y. J., Kim, E., Park, J. W., Sherman, D. H., Gerwick, W. H., and Yoon, Y. J. (2012) Heterologous Production of 4-O-Demethylbarbamide, a Marine Cyanobacterial Natural Product. *Org. Lett.* 14, 5824–5827.
- (11) Ziemert, N., Ishida, K., Liaimer, A., Hertweck, C., and Dittmann, E. (2008) Ribosomal Synthesis of Tricyclic Depsipeptides in Bloom-Forming Cyanobacteria. *Angew. Chem., Int. Ed.* 47, 7756–7759.
- (12) Liu, T., Mazmouz, R., Ongley, S. E., Chau, R., Pickford, R., Woodhouse, J. N., and Neilan, B. A. (2017) Directing the Heterologous Production of Specific Cyanobacterial Toxin Variants. *ACS Chem. Biol.* 12, 2021–2029.
- (13) Tianero, M. D. B., Donia, M. S., Young, T. S., Schultz, P. G., and Schmidt, E. W. (2012) Ribosomal Route to Small-Molecule Diversity. *J. Am. Chem. Soc.* 134, 418–425.
- (14) Ongley, S. E., Bian, X., Zhang, Y., Chau, R., Gerwick, W. H., Müller, R., and Neilan, B. A. (2013) High-Titer Heterologous Production in *E. coli* of Lyngbyatoxin, a Protein Kinase C Activator from an Uncultured Marine Cyanobacterium. *ACS Chem. Biol.* 8, 1888–1893.
- (15) Videau, P., Wells, K. N., Singh, A. J., Gerwick, W. H., and Philmus, B. (2016) Assessment of *Anabaena* sp. Strain PCC 7120 as a Heterologous Expression Host for Cyanobacterial Natural Products: Production of Lyngbyatoxin A. *ACS Synth. Biol.* 5, 978.
- (16) Yang, G., Cozad, M. A., Holland, D. A., Zhang, Y., Luesch, H., and Ding, Y. (2018) Photosynthetic Production of Sunscreen Shinorine Using an Engineered Cyanobacterium. *ACS Synth. Biol.* 7, 664–671.
- (17) Lassen, L. M., Nielsen, A. Z., Ziersen, B., Gnanasekaran, T., Møller, B. L., and Jensen, P. E. (2014) Redirecting Photosynthetic Electron Flow into Light-Driven Synthesis of Alternative Products Including High-Value Bioactive Natural Compounds. *ACS Synth. Biol.* 3, 1–12.
- (18) Englund, E., Andersen-Ranberg, J., Miao, R., Hamberger, B., and Lindberg, P. (2015) Metabolic Engineering of *Synechocystis* sp. PCC 6803 for Production of the Plant Diterpenoid Manoyl Oxide. *ACS Synth. Biol.* 4, 1270–1278.
- (19) Włodarczyk, A., Gnanasekaran, T., Nielsen, A. Z., Zulu, N. N., Mellor, S. B., Luckner, M., Thøfner, J. F. B., Olsen, C. E., Mottawie, M. S., Burrow, M., Pribil, M., Feussner, I., Møller, B. L., and Jensen, P. E. (2016) Metabolic engineering of light-driven cytochrome P450 dependent pathways into *Synechocystis* sp. PCC 6803. *Metab. Eng.* 33, 1–11.
- (20) Xue, Y., Zhang, Y., Grace, S., and He, Q. (2014) Functional expression of an *Arabidopsis* p450 enzyme, p-coumarate-3-hydroxylase, in the cyanobacterium *Synechocystis* PCC 6803 for the biosynthesis of caffeic acid. *J. Appl. Phycol.* 26, 219–226.
- (21) Lassen, L. M., Nielsen, A. Z., Olsen, C. E., Bialek, W., Jensen, K., Møller, B. L., and Jensen, P. E. (2014) Anchoring a plant cytochrome P450 via PsaM to the thylakoids in *Synechococcus* sp. PCC 7002: Evidence for light-driven biosynthesis. *PLoS One* 9, e102184.
- (22) Yu, J., Liberton, M., Cliften, P. F., Head, R. D., Jacobs, J. M., Smith, R. D., Koppelaar, D. W., Brand, J. J., and Pakrasi, H. B. (2015) *Synechococcus elongatus* UTEX 2973, a fast growing cyanobacterial chassis for biosynthesis using light and CO₂. *Sci. Rep.* 5, 8132.
- (23) Jaiswal, D., Sengupta, A., Sohoni, S., Sengupta, S., Phadnavis, A. G., Pakrasi, H. B., and Wangikar, P. P. (2018) Genome Features and Biochemical Characteristics of a Robust, Fast Growing and Naturally Transformable Cyanobacterium *Synechococcus elongatus* PCC 11801 Isolated from India. *Sci. Rep.* 8, 16632.
- (24) Walton, K., and Berry, P. J. (2016) Indole Alkaloids of the Stigonematales (Cyanophyta): Chemical Diversity, Biosynthesis and Biological Activity. *Mar. Drugs* 14, 73.
- (25) Acuña, U. M., Mo, S., Zi, J., Orjala, J., and De Blanco, E. J. C. (2018) Hapalindole H Induces Apoptosis as an Inhibitor of NF-κB and Affects the Intrinsic Mitochondrial Pathway in PC-3 Androgen-insensitive Prostate Cancer Cells. *Anticancer Res.* 38, 3299–3307.
- (26) Kim, H., Lantvit, D., Hwang, C. H., Kroll, D. J., Swanson, S. M., Franzblau, S. G., and Orjala, J. (2012) Indole alkaloids from two cultured cyanobacteria, *Westiellopsis* sp. and *Fischerella muscicola*. *Bioorg. Med. Chem.* 20, 5290–5295.

- (27) Mo, S., Kronic, A., Chlipala, G., and Orjala, J. (2009) Antimicrobial ambigaine isonitriles from the cyanobacterium *Fischerella ambigua*. *J. Nat. Prod.* 72, 894–899.
- (28) Micallef, M. L., Sharma, D., Bunn, B. M., Gerwick, L., Viswanathan, R., and Moffitt, M. C. (2014) Comparative analysis of hapalindole, ambigaine and welwitindolinone gene clusters and reconstitution of indole–isonitrile biosynthesis from cyanobacteria. *BMC Microbiol.* 14, 213.
- (29) Hillwig, M. L., Zhu, Q., and Liu, X. (2014) Biosynthesis of Ambiguine Indole Alkaloids in Cyanobacterium *Fischerella ambigua*. *ACS Chem. Biol.* 9, 372–377.
- (30) Li, S., Lowell, A. N., Yu, F., Raveh, A., Newmister, S. A., Bair, N., Schaub, J. M., Williams, R. M., and Sherman, D. H. (2015) Hapalindole/Ambiguine Biogenesis Is Mediated by a Cope Rearrangement, C-C Bond-Forming Cascade. *J. Am. Chem. Soc.* 137, 15366–15369.
- (31) Liu, X., Hillwig, M. L., Koharudin, L. M. I., and Gronenborn, A. M. (2016) Unified biogenesis of ambigaine, fischerindole, hapalindole and welwitindolinone: identification of a monogeranylated indolenine as a cryptic common biosynthetic intermediate by an unusual magnesium-dependent aromatic prenyltransferase. *Chem. Commun.* 52, 1737–1740.
- (32) Li, S., Lowell, A. N., Newmister, S. A., Yu, F., Williams, R. M., and Sherman, D. H. (2017) Decoding cyclase-dependent assembly of hapalindole and fischerindole alkaloids. *Nat. Chem. Biol.* 13, 467.
- (33) Newmister, S. A., Li, S., Garcia-Borràs, M., Sanders, J. N., Yang, S., Lowell, A. N., Yu, F., Smith, J. L., Williams, R. M., Houk, K. N., and Sherman, D. H. (2018) Structural basis of the Cope rearrangement and cyclization in hapalindole biogenesis. *Nat. Chem. Biol.* 14, 345–351.
- (34) Brady, S. F., and Clardy, J. (2005) Systematic Investigation of the *Escherichia coli* Metabolome for the Biosynthetic Origin of an Isocyanide Carbon Atom. *Angew. Chem.* 117, 7207–7210.
- (35) Zhu, Q., and Liu, X. (2017) Discovery of a Calcium-Dependent Enzymatic Cascade for the Selective Assembly of Hapalindole-Type Alkaloids: On the Biosynthetic Origin of Hapalindole U. *Angew. Chem., Int. Ed.* 56, 9062–9066.
- (36) Hillwig, M. L., Zhu, Q., Ittiarnkul, K., and Liu, X. (2016) Discovery of a Promiscuous Non-Heme Iron Halogenase in Ambiguine Alkaloid Biogenesis: Implication for an Evolvable Enzyme Family for Late-Stage Halogenation of Aliphatic Carbons in Small Molecules. *Angew. Chem., Int. Ed.* 55, 5780–5784.
- (37) Hillwig, M. L., and Liu, X. (2014) A new family of iron-dependent halogenases acts on freestanding substrates. *Nat. Chem. Biol.* 10, 921.
- (38) Wong, C. P., Awakawa, T., Nakashima, Y., Mori, T., Zhu, Q., Liu, X., and Abe, I. (2018) Two Distinct Substrate Binding Modes for the Normal and Reverse Prenylation of Hapalindoles by the Prenyltransferase AmbP3. *Angew. Chem., Int. Ed.* 57, 560–563.
- (39) Ungerer, J., Lin, P.-C., Chen, H.-Y., and Pakrasi, H. B. (2018) Adjustments to Photosystem Stoichiometry and Electron Transfer Proteins Are Key to the Remarkably Fast Growth of the Cyanobacterium *Synechococcus elongatus* UTEX 2973. *mBio* 9, e02327–02317.
- (40) Sleight, S. C., Bartley, B. A., Lieviant, J. A., and Sauro, H. M. (2010) Designing and engineering evolutionary robust genetic circuits. *J. Biol. Eng.* 4, 12–12.
- (41) Choi, S. Y., Park, B., Choi, I.-G., Sim, S. J., Lee, S.-M., Um, Y., and Woo, H. M. (2016) Transcriptome landscape of *Synechococcus elongatus* PCC 7942 for nitrogen starvation responses using RNA-seq. *Sci. Rep.* 6, 30584.
- (42) Camsund, D., and Lindblad, P. (2014) Engineered transcriptional systems for cyanobacterial biotechnology. *Front. Bioeng. Biotechnol.* 2, 40.
- (43) Berla, B. M., Saha, R., Immethun, C. M., Maranas, C. D., Moon, T. S., and Pakrasi, H. B. (2013) Synthetic biology of cyanobacteria: unique challenges and opportunities. *Front. Microbiol.* 4, 1–14.
- (44) Knoot, C. J., and Pakrasi, H. B. (2019) Diverse hydrocarbon biosynthetic enzymes can substitute for olefin synthase in the cyanobacterium *Synechococcus* sp. PCC 7002. *Sci. Rep.* 9, 1360.
- (45) Brady, S. F., and Clardy, J. (2005) Cloning and Heterologous Expression of Isocyanide Biosynthetic Genes from Environmental DNA. *Angew. Chem., Int. Ed.* 44, 7063–7065.
- (46) Taton, A., Unglaub, F., Wright, N. E., Zeng, W. Y. u., Paz-Yepes, J., Brahamsha, B., Palenik, B., Peterson, T. C., Haerizadeh, F., Golden, S. S., and Golden, J. W. (2014) Broad-host-range vector system for synthetic biology and biotechnology in cyanobacteria. *Nucleic Acids Res.* 42, e136.
- (47) Ungerer, J., and Pakrasi, H. B. (2016) Cpf1 Is A Versatile Tool for CRISPR Genome Editing Across Diverse Species of Cyanobacteria. *Sci. Rep.* 6, 39681.
- (48) Gatti-Lafronconi, P., Dijkman, W. P., Devenish, S. R. A., and Hollfelder, F. (2013) A single mutation in the core domain of the lac repressor reduces leakiness. *Microb. Cell Fact.* 12, 67.
- (49) Chen, C.-C., Hu, X., Tang, X., Yang, Y., Ko, T.-P., Gao, J., Zheng, Y., Huang, J.-W., Yu, Z., Li, L., Han, S., Cai, N., Zhang, Y., Liu, W., and Guo, R.-T. (2018) The Crystal Structure of a Class of Cyclases that Catalyze the Cope Rearrangement. *Angew. Chem., Int. Ed.* 57, 15060–15064.
- (50) Awakawa, T., Mori, T., Nakashima, Y., Zhai, R., Wong, C. P., Hillwig, M. L., Liu, X., and Abe, I. (2018) Molecular Insight into the Mg²⁺-Dependent Allosteric Control of Indole Prenylation by Aromatic Prenyltransferase AmbP1. *Angew. Chem., Int. Ed.* 57, 6810–6813.
- (51) Lin, P.-C., and Pakrasi, H. B. (2019) Engineering cyanobacteria for production of terpenoids. *Planta* 249, 145.
- (52) Wendt, K. E., Ungerer, J., Cobb, R. E., Zhao, H., and Pakrasi, H. B. (2016) CRISPR/Cas9 mediated targeted mutagenesis of the fast growing cyanobacterium *Synechococcus elongatus* UTEX 2973. *Microb. Cell Fact.* 15, 115.
- (53) Li, S., Sun, T., Xu, C., Chen, L., and Zhang, W. (2018) Development and optimization of genetic toolboxes for a fast-growing cyanobacterium *Synechococcus elongatus* UTEX 2973. *Metab. Eng.* 48, 163–174.
- (54) Aversch, N. J. H., and Krömer, J. O. (2018) Metabolic Engineering of the Shikimate Pathway for Production of Aromatics and Derived Compounds—Present and Future Strain Construction Strategies. *Front. Bioeng. Biotechnol.* 6, 32.
- (55) Oliver, N. J., Rabinovitch-Deere, C. A., Carroll, A. L., Nozzi, N. E., Case, A. E., and Atsumi, S. (2016) Cyanobacterial metabolic engineering for biofuel and chemical production. *Curr. Opin. Chem. Biol.* 35, 43–50.
- (56) Knoot, C. J., Ungerer, J., Wangikar, P. P., and Pakrasi, H. B. (2018) Cyanobacteria: Promising biocatalysts for sustainable chemical production. *J. Biol. Chem.* 293, 5044–5052.
- (57) Gibson, D. G., Young, L., Chuang, R.-Y., Venter, J. C., Hutchison, C. A., III, and Smith, H. O. (2009) Enzymatic assembly of DNA molecules up to several hundred kilobases. *Nat. Methods* 6, 343.
- (58) Landry, B. P., Palanki, R., Dylguyarov, N., Hartsough, L. A., and Tabor, J. J. (2018) Phosphatase activity tunes two-component system sensor detection threshold. *Nat. Commun.* 9, 1433.
- (59) Espah Borujeni, A., Channarasappa, A. S., and Salis, H. M. (2014) Translation rate is controlled by coupled trade-offs between site accessibility, selective RNA unfolding and sliding at upstream standby sites. *Nucleic Acids Res.* 42, 2646–2659.
- (60) Davison, V. J., Woodside, A. B., Neal, T. R., Stremler, K. E., Muehlbacher, M., and Poulter, C. D. (1986) Phosphorylation of isoprenoid alcohols. *J. Org. Chem.* 51, 4768–4779.